Available online at www.sciencedirect.com

Catalysis Today 116 (2006) 361–366

www.elsevier.com/locate/cattod

Low-temperature steam-reforming of ethanol over ZnO-supported Ni and Cu catalysts

The effect of nickel and copper addition to ZnO-supported cobalt-based catalysts

Narcís Homs, Jordi Llorca [1], Pilar Ramírez de la Piscina *

Departament de Química Inorgànica, Universitat de Barcelona, C/Martí i Franquès 1-11, 08028 Barcelona, Spain

Abstract

ZnO-supported Ni and Cu as well as bimetallic Co-Ni and Co-Cu catalysts containing ca. 0.7 wt% sodium promoter and prepared by the co-precipitation method were tested in the ethanol steam-reforming reaction at low temperature (523–723 K), using a bioethanol-like mixture diluted in Ar. Monometallic ZnO-supported Cu or Ni samples do not exhibit good catalytic performance in the steam-reforming of ethanol for hydrogen production. Copper catalyst mainly dehydrogenates ethanol to acetaldehyde, whereas nickel catalyst favours ethanol decomposition. However, the addition of Ni to ZnO-supported cobalt has a positive effect both on the production of hydrogen at low temperature (<573 K), and on catalyst stability. Evidence for alloy formation as well as mixed oxides at the microstructural level was found in the bimetallic systems after running the ethanol steam-reforming reaction by HRTEM–EELS.

Keywords: Ethanol-reforming; Hydrogen; Bimetallic catalysts; Nickel catalysts; Copper catalysts

1. Introduction

The use of a renewable, non-toxic biomass-derived source, like bioethanol, to produce hydrogen is currently very attractive. In this domain, the search for a highly effective catalytic system for the selective steam-reforming process is of high research interest:

$$CH_3CH_2OH + 3H_2O \rightarrow 6H_2 + 2CO_2$$

Besides noble metal-based systems, the reaction has been studied extensively over supported Ni [1–8], Cu [6], Ni–Cu [9,10] and Co [11–17]. From the data reported, not only the metal phase, but also the support used has been shown to influence the catalytic performance [18]. The steam-reforming of ethanol involves numerous steps and usually competes with several parallel reactions that originate undesired products that result in lower hydrogen yields and create difficulties for practical applications. Undesired products like CO and CH_4 must be further processed in order to be removed, with additional energy cost. On the other hand, a major concern in the steam-reforming reaction of ethanol is the deactivation of catalysts, which mainly takes place via carbon deposition. Recently, we have shown that sodium addition to ZnO-supported cobalt catalysts promotes the steam-reforming of ethanol [15]. The promotion has been related to the increasing of H_2 yield and the stability of catalysts by suppressing the deposition of carbon. Taking into account these considerations and the well-documented state of the art of the reaction with Ni- and Cu-based systems, the present article reports our study of ZnO-supported Ni and Cu catalysts as well as the effect of Ni or Cu addition on the Na-promoted, Co-ZnO system. The catalysts were characterised by means of X-ray diffraction (XRD), X-ray photoelectron spectroscopy (XPS), high-resolution transmission electron microscopy (HRTEM) and electron energy loss spectroscopy (EELS) and tested in the steam-reforming reaction of bioethanol-like mixtures.

---

* Corresponding author. Tel.: +34 934037056; fax: +34 934907725. *E-mail address:* pilar.piscina@qi.ub.es (P.R. de la Piscina).

[1] Present address: Institut de Tècniques Energètiques, Universitat Politècnica de Catalunya, Diagonal 647, 08028 Barcelona, Spain.

0920-5861/$ – see front matter © 2006 Elsevier B.V. All rights reserved.
doi:10.1016/j.cattod.2006.05.081

Table 1
Chemical analysis (wt%) and BET surface areas of catalysts

Catalyst	Co (%)	Ni (%)	Cu (%)	Na (%)	($m^2\ g^{-1}$)
10Co1Ni(Na)-ZnO	9.40	0.95	–	0.64	41.4
10Co1Cu(Na)-ZnO	9.30	–	0.93	0.78	39.7
10Co(Na)-ZnO	10.7	–	–	0.78	36.2
10Ni/ZnO	–	10.9	–	–	47.9
10Cu/ZnO	–	–	10.4	–	46.8

2. Experimental methods

Bimetallic catalysts with a cobalt content of ca. 10 wt%, Ni or Cu content of ca. 1 wt%, and sodium content of ca. 0.7 wt% were prepared by the co-precipitation method. Precipitation was accomplished at 313 K by the addition of a Na_2CO_3 solution to $Zn(NO_3)_2$ and $Co(NO_3)_2$, and $Ni(NO_3)_2$ or $Cu(NO_3)_2$ aqueous solutions. After ageing at 313 K for 1.5 h, the suspensions were filtered and the filtrates washed with distilled water. The resulting solids were then dried at 363 K overnight and calcined in air at 673 K for 12 h. Samples were reduced under hydrogen at 673 K for 12 h and labelled as 10Co1M(Na)-ZnO (M = Ni, Cu). As reference, a sodium-promoted cobalt catalyst, 10Co(Na)-ZnO, was prepared similarly [15]. For comparative purposes, monometallic ZnO-supported Ni and Cu catalysts were prepared by impregnation from their respective nitrates on ZnO. The support was prepared by decomposition of $3ZnO{\cdot}2ZnCO_3{\cdot}3H_2O$ under Ar at 573 K. The salts were impregnated by the incipient wetness method from aqueous solutions. Samples were dried at 373 K for 6 h, calcined at 673 K for 6 h, and reduced under H_2 at 673 K. The resulting catalysts were labelled as 10M/ZnO (M = Ni, Cu). Table 1 compiles the chemical composition obtained by optical emission spectroscopy with inductively-coupled plasma (ICP-OES, Perkin-Elmer Optima apparatus) and BET surface area determined using a Micromeritics ASAP 9000 instrument of all samples. X-ray diffraction profiles were collected at a step width of 0.02° and by counting 10 s at each step with a Siemens D-500 instrument equipped with a Cu target and a graphite monochromator. Photoelectron spectra (XPS) were acquired with a Perkin-Elmer PHI-5500 spectrometer equipped with an Al X-ray exciting source and a hemispherical electron analyser. High-resolution transmission electron microscopy and electron energy loss spectroscopy was performed with a JEOL JEM 2010F instrument working at 200 kV and equipped with a field emission source. Catalytic studies of ethanol steam-reforming were performed at atmospheric pressure in a U-shaped quartz reactor (5 mm internal diameter). 0.1–0.2 g of catalyst were charged and diluted with inactive SiC, giving a catalyst bed volume of 0.6 ml. A constant mixture of $C_2H_5OH:H_2O = 1:4$ (v/v) ($C_2H_5OH:H_2O \sim 1:13$ molar basis, HPLC purity grade) was supplied by a Gilson 307 Piston Pump and vaporised at 453 K. The temperature of the catalyst was first raised under Ar to that of the first temperature tested, and then the Ar stream was mixed with the $C_2H_5OH + H_2O$ mixture ($(C_2H_5OH + H_2O):Ar = 1:5$ molar basis). The GHSV was 5000 h^{-1} in all cases. At the end of the catalytic tests, the flow of $C_2H_5OH + H_2O$ was stopped and the catalysts were cooled under Ar stream and stored for characterisation. The analysis of the reactants and all the reaction products was carried out on-line by gas chromatography as described previously [12]. The detection limit of CO was ca. 20 ppm. Response factors for all products were obtained with appropriate standards before and after each catalytic test. The selectivity of the products was calculated on the basis of molar percentage of each product evolved (water excluded) with respect to the total moles of products formed.

3. Results and discussion

3.1. Monometallic catalysts

In this section, we evaluate the catalytic behaviour of monometallic ZnO-supported nickel and copper catalysts, and discuss their bulk structural characteristics from X-ray

Table 2
Catalytic performance of 10M/ZnO (M = Cu, Ni) in the ethanol steam-reforming reaction

Catalyst	*T* (K)	*t* (h)	Conversion (%)	Activity[a] (mol C_2H_5OH/mol M h)	Selectivity[b] (%)								mol H_2/mol EtOH[c]	mol CO_2/mol EtOH[c]
					H_2	CO	CO_2	CH_4	C_2H_4	C_3H_6	CH_3CHO	Me_2CO		
10Cu/ZnO	573	2	<1	–	–	–	–	–	–	–	–	–	–	–
	623	4	3.0	0.17	52.4	–	0.3	–	3.1	–	44.2	–	0.03	0.00
	673	6	21.1	1.22	53.6	–	1.1	–	3.2	–	42.1	–	0.25	0.01
	673	26	18.5	1.07	52.1	–	1.5	0.1	2.4	0.1	43.3	0.5	0.20	0.01
	723	28	82.2	4.77	56.2	–	8.3	0.5	1.9	0.5	24.8	7.8	1.06	0.16
	723	48	84.1	4.88	58.6	–	9.0	1.2	0.9	0.4	23.0	7.0	1.23	0.19
10Ni/ZnO	573	2	77.3	4.27	47.6	15.9	6.3	15.3	0.1	–	14.7	–	1.09	0.14
	623	4	100	n.a.	54.2	–	25.0	20.7	0.2	–	–	–	2.35	1.09
	673	6	100	n.a.	55.6	–	25.0	19.4	–	–	–	–	2.50	1.12
	673	26	100	n.a.	65.1	–	25.0	9.9	–	–	–	–	3.73	1.43
	723	28	100	n.a.	64.5	1.2	24.0	10.2	–	–	–	–	3.64	1.35
	723	48	100	n.a.	66.5	1.3	23.8	8.4	–	–	–	–	3.96	1.42

$C_2H_5OH:H_2O:Ar = 1:13:70$ (molar ratio); GHSV = 5000 h^{-1}; 0.1 g of catalyst.

[a] n.a., Non-applied.

[b] Molar percentage of products (water excluded).

[c] Corresponds to ethanol in the reactant mixture.

diffraction profiles recorded before and after reaction. Catalytic results are compiled in Table 2.

Under the reaction conditions used, 10Cu/ZnO material is a poor catalyst. Below 723 K, ethanol conversion is less than 20% and the main product besides hydrogen is acetaldehyde, thus indicating that it behaves as a dehydrogenation catalyst, favouring the reaction:

$$CH_3CH_2OH \rightarrow CH_3CHO + H_2$$

In contrast, 10Ni/ZnO is a very active catalyst and full ethanol conversion is achieved already at 623 K. However, products are almost exclusively H_2, CO_2 and CH_4. This seems to indicate that the decomposition reaction of ethanol over this catalyst is clearly favoured:

$$CH_3CH_2OH \rightarrow CH_4 + H_2 + CO$$

and the large excess of water present in the bioethanol-like mixture used favours the water gas shift reaction (WGSR), at least up to 723 K:

$$CO + H_2O \rightarrow H_2 + CO_2$$

Also, at higher temperatures there is a decrease of methane selectivity which could be related to the concurrence of additional reactions such as:

$$CH_4 + H_2O \rightarrow 3H_2 + CO$$

Concerning the structural characteristics of catalysts, Fig. 1 shows the X-ray diffractograms recorded for the 10Cu/ZnO catalyst before and after the reduction treatment as well as after the catalytic test. Before reduction (Fig. 1a), diffraction peaks due to the CuO phase appear at 35.5, 38.9, 48.8, 58.3 and 61.7°. After reduction at 673 K (Fig. 1b), all the diffraction peaks of CuO disappear and new peaks appear at 42.9 and 49.8° which correspond to Cu alloyed with Zn. However, after the reaction test at 723 K (Fig. 1c), the diffraction lines at 43.3 and 50.3° indicate that metallic Cu is the dominant crystalline phase visible by X-ray diffraction, although some minor amount of Cu–Zn alloy is still visible. There are no diffraction peaks corresponding to Cu oxides.

The X-ray diffractogram recorded for the 10Ni/ZnO catalyst before the reduction treatment (Fig. 2a) shows the presence of the NiO phase (peaks at 37.2 and 43.2°). After the reduction treatment at 673 K (Fig. 2b), several Ni–Zn alloys develop (lines at 43.7, 44.2, 46.9 and 51.2°) and there are still diffraction lines due to NiO. However, the diffractogram recorded after the catalytic test at 723 K (Fig. 2c) only contains diffraction lines of metallic nickel at 44.5 and 51.9°.

3.2. Bimetallic catalysts

The catalytic results obtained from ethanol steam-reforming tests performed over the ZnO-supported and Na-promoted bimetallic Co-Cu and Co-Ni catalysts are compiled in Table 3. For comparative purposes, Table 3 also contains a summary of the catalytic performance of 10Co(Na)-ZnO catalyst which has been previously reported in detail [15]. The temperature of the catalytic tests has been raised from 523 up to 723 K and, after that, decreased down to 523 K in order to check for catalyst deactivation. There is a clear improvement in the catalytic performance of the 10Co1Ni(Na)-ZnO and 10Co1Cu(Na)-ZnO catalysts with respect to the monometallic 10Ni/ZnO and 10Cu/ZnO, respectively, both in terms of activity and selectivity to reforming products (see Tables 2 and 3). On the other hand, the most remarkable effect of the addition of nickel to cobalt with

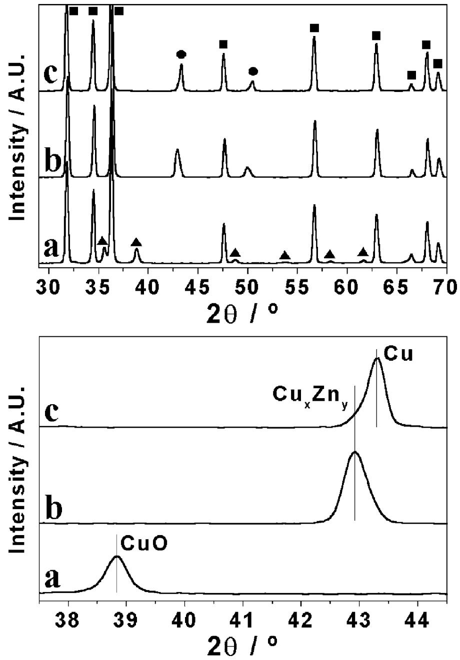

Fig. 1. X-ray diffraction profiles of sample 10Cu/ZnO before reduction (a), after reduction at 673 K (b), and after ethanol steam-reforming (c). (■) ZnO; (▲) CuO; (●) Cu.

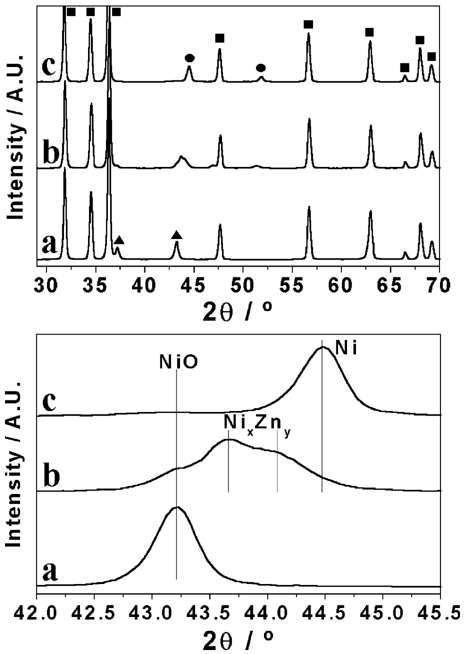

Fig. 2. X-ray diffraction profiles of sample 10Ni/ZnO before reduction (a), after reduction at 673 K (b), and after ethanol steam-reforming (c). (■) ZnO; (▲) NiO; (●) Ni.

Table 3
Catalytic performance of 10Co1M(Na)-ZnO (M = Cu, Ni) in the ethanol steam-reforming reaction

Catalyst	T (K)	t (h)	Conversion (%)	Activity[a] (mol C_2H_5OH/mol (Co + M) h)	Selectivity[b] (%)						(mol H_2/mol EtOH)[c]	(mol CO_2/mol EtOH)[c]
					H_2	CO	CO_2	CH_4	C_2H_4	CH_3CHO		
10Co1Cu(Na)-ZnO	523	2	3.9	0.23	51.2	–	–	–	–	48.8	0.04	–
	573	4	74.1	4.36	70.8	–	23.7	2.8	0.3	2.3	3.29	1.10
	573	24	74.3	4.37	70.8	–	23.9	3.1	0.1	2.1	3.35	1.13
	623	26	100	n.a.	72.2	–	25.0	2.8	–	–	5.19	1.80
	673	28	100	n.a.	73.0	–	24.9	2.1	–	–	5.41	1.85
	723	30	100	n.a.	73.2	0.2	24.9	1.7	–	–	5.46	1.85
	723	50	100	n.a.	73.4	–	25.0	1.5	–	–	5.53	1.88
	573	52	70.2	4.14	70.9	–	23.2	2.4	–	3.5	3.05	1.00
	523	54	5.4	0.32	50.6	–	–	–	–	49.4	0.06	–
10Co1Ni(Na)-ZnO	523	2	4.1	0.24	50.4	–	–	–	–	49.6	0.04	–
	573	4	89.9	5.23	68.1	–	25.0	6.9	–	–	3.84	1.41
	573	24	91.0	5.29	68.3	–	25.0	6.7	–	–	3.93	1.43
	623	26	100	n.a.	64.5	–	25.1	10.5	–	–	3.63	1.41
	673	28	100	n.a.	67.5	–	24.9	7.6	–	–	4.15	1.53
	723	30	100	n.a.	60.5	1.0	23.9	14.6	–	–	3.07	1.21
	723	50	100	n.a.	66.2	–	25.0	8.8	–	–	3.92	1.48
	573	52	90.8	5.29	67.9	–	25.0	7.1	–	–	3.84	1.41
	523	54	7.4	0.43	46.8	–	–	3.2	–	50.0	0.07	–
10Co(Na)-ZnO[d]	523	2	1.4	0.08	50.4	–	–	–	–	49.6	0.01	–
	573	4	66.3	3.73	73.0	–	24.4	1.2	–	1.5	3.39	1.13
	573	24	66.5	3.74	73.1	–	24.2	1.1	–	1.6	3.41	1.13

$C_2H_5OH:H_2O:Ar = 1:13:70$ (molar ratio); GHSV = 5000 h^{-1}; 0.1 g of catalyst.

[a] n.a., Non-applied.

[b] Molar percentage of products (water excluded).

[c] Corresponds to ethanol in the reactant mixture.

[d] Data from Ref. [15].

respect to monometallic cobalt-based catalyst is an increase in activity values at low reaction temperatures (523 and 573 K), which results in a higher yield of hydrogen production: 3.9 mol H_2 per mol EtOH versus 3.4 mol H_2 per mol EtOH introduced for 10Co1Ni(Na)-ZnO and 10Co(Na)-ZnO after 24 h on stream at 573 K, respectively (Table 3). The activity of catalyst 10Co1Cu(Na)-ZnO is also higher than that of 10Co(Na)-ZnO, but the poorer selectivity to reforming products of the former results in a similar production of hydrogen for both catalysts.

Concerning the stability of the bimetallic catalysts, when the sample 10Co1Cu(Na)-ZnO has been held for 20 h at 723 K, there is a decrease in the activity at 573 K in comparison with the initial value at this temperature (Table 3), whereas no deactivation occurs over the 10Co1Ni(Na)-ZnO catalyst after the same treatment. In fact, the deactivation for 10Co1Ni(Na)-ZnO is even lower than that reported for 10Co(Na)-ZnO [15]. The deactivation of 10Co1Cu(Na)-ZnO may be related to the build-up of carbonaceous deposits, as is illustrated by XPS measurements (ΔC column in Table 4).

The X-ray diffraction characterisation of catalysts (not shown) points to the presence of diffraction peaks due mainly to metallic cobalt, although the possibility of alloying and the presence of metal oxides cannot be ruled out. The characterisation of samples by X-ray photoelectron spectroscopy before and after ethanol steam-reforming is resumed in Table 4. It can be deduced that the surface composition of samples before and after reaction do not substantially differ. A slight enrichment of copper or nickel on the surface of the catalysts is observed in the bimetallic samples. In all cases there is a significant segregation of sodium on surface.

In order to gain further insight into the microstructural characteristics of the bimetallic samples after ethanol steam-reforming, a detailed HRTEM–EELS study was performed. Fig. 3 shows a representative HRTEM image of catalyst 10Co1Cu(Na)-ZnO along with Fourier transform images of selected areas. Area labelled ‘a’ corresponds to the ZnO support (lattice fringes at 2.81 and 2.48 Å for (1 0 0) and (1 0 1) planes, respectively). The particle on top of ZnO exhibits a complex high-resolution pattern. The Fourier transform image of area labelled ‘b’ contains spots at 4.68 and 2.87 Å in addition to ZnO spots, which may correspond to a $Co_{3-x}Cu_xO_4$ phase (values at 4.68 and 2.87 Å are exactly

Table 4
Surface atomic ratios from X-ray photoelectron spectroscopy of several catalysts as prepared and after ethanol steam-reforming

Catalyst	Co_{at}/Zn_{at}		Na_{at}/Co_{at}		M_{at}/Co_{at}[a]		ΔC[b]
	Before	After	Before	After	Before	After	
10Co(Na)-ZnO	0.30	0.24	1.09	0.97	–	–	0.33
10Co1Ni(Na)-ZnO	0.26	0.24	0.97	1.10	0.19	0.17	0.20
10Co1Cu(Na)-ZnO	0.32	0.36	0.97	1.05	0.17	0.12	2.41

[a] M = Ni, Cu.

[b] $(C_{at}/Co_{at})_{\text{after reaction}} - (C_{at}/Co_{at})_{\text{before reaction}}$.

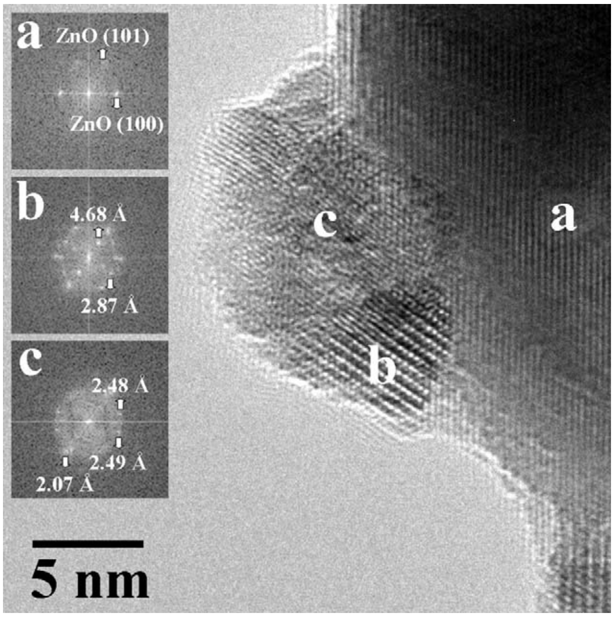

Fig. 3. High-resolution transmission electron microscopy image of catalyst 10Co1Cu(Na)-ZnO after ethanol steam-reforming. Fourier transform images of selected areas labelled a, b, and c are included.

encountered for $Co_{2.08}Cu_{0.92}O_4$, JCPDS-ICDD 37-0878). The Fourier transform image of the area labelled 'c' contains spots at 2.49, 2.48, and 2.07 Å. The value at 2.07 Å is in agreement with (1 1 1) planes of metallic Co-Cu solid solutions (JCPDS-ICDD 50-1452), whereas the spots at 2.48–2.49 Å are unspecific and may correspond to a variety of mixed Co-Cu oxides or even Cu oxide alone.

Fig. 4 shows a representative HRTEM image of catalyst 10Co1Ni(Na)/ZnO. Again, a quite complex lattice fringe pattern is observed for the particles on ZnO. The insets of Fig. 4 correspond to the electron energy loss spectrum and Fourier transform image of the marked area. From EELS it is deduced that cobalt and nickel are both present in the area encircled. Spots in the Fourier transform image at 4.70 Å can be explained by the presence of (1 1 1) planes of a Co-Ni oxide with $Fd3m$ space group ($Co_{1.29}Ni_{1.71}O_4$; JCPDS-ICDD 40-1191), and those at 4.05 Å correspond to (0 0 1) planes of hexagonal metallic cobalt. Finally, spots at 4.63–4.65 and 4.86 Å are again unspecific, but point to the presence of Co-Ni mixed oxides.

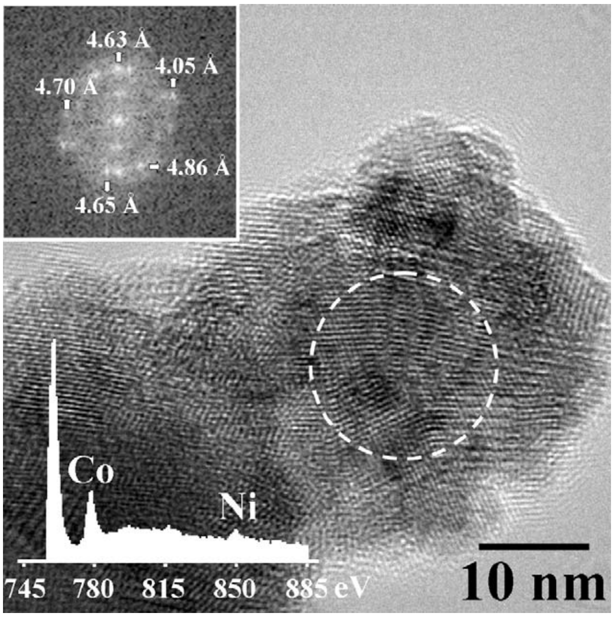

Fig. 4. High-resolution transmission electron microscopy image of catalyst 10Co1Ni(Na)-ZnO after ethanol steam-reforming. The EEL spectrum and Fourier transform image of the circled area are included.

The characterization results point to the formation of $Co_{3-x}M_xO_4$ mixed oxide particles (M = Ni, Cu) after the calcination of catalysts, these particles may evolve to metallic aggregates containing Co-M solid solutions after reduction.

4. Conclusions

Neither copper nor nickel alone supported on zinc oxide appear as appropriate catalysts for the steam-reforming of bioethanol under desired low temperature conditions for hydrogen production. Over the copper sample dehydrogenation of ethanol into acetaldehyde occurs but the reforming reaction does not further progress significantly into H_2 and CO_x. On the other hand, over the nickel sample the decomposition reaction of ethanol to CH_4 and CO_x is favoured. Only at high temperature can the methane production be lowered through steam-reforming. The yield of H_2 production is improved over ZnO-supported, Na-promoted Co-Ni sample with respect to Co catalysts at low temperatures due to an increase of catalytic activity. No significant improvement is observed over a similar Co-Cu sample. Mixed oxides and as well as metallic solid solutions are present at the nanoscale level after ethanol steam-reforming.

Acknowledgements

We thank MCYT (MAT 2002-01739, MAT 2005-03456) and CIRIT (2005SGR-00184) for financial support. J.L. is grateful to MCYT for a Ramon y Cajal research program and DURSI (Generalitat de Catalunya).

References

[1] A.N. Fatsikostas, D.I. Kondarides, X.E. Verykios, Chem. Commun. (2001) 851.
[2] A.N. Fatsikostas, D.I. Kondarides, X.E. Verykios, Catal. Today 75 (2002) 145.
[3] A.N. Fatsikostas, X.E. Verykios, J. Catal. 225 (2004) 439.
[4] F. Frusteri, S. Freni, V. Chiodo, L. Spadaro, O. Di Blasi, G. Bonura, S. Cavallaro, Appl. Catal. A: Gen. 270 (2004) 1.
[5] J.P. Breen, R. Burch, H.M. Coleman, Appl. Catal. B: Environ. 39 (2002) 65.
[6] F. Auprêtre, C. Descorme, D. Duprez, Catal. Commun. 3 (2002) 267.
[7] S. Freni, S. Cavallaro, N. Mondello, L. Spadaro, F. Frusteri, Catal. Commun. 4 (2003) 259.
[8] F. Frusteri, S. Freni, L. Spadaro, V. Chiodo, G. Bonura, S. Donato, S. Cavallaro, Catal. Commun. 5 (2004) 611.
[9] V. Fierro, V. Klouz, O. Akdim, C. Mirodatos, Catal. Today 75 (2002) 141.

[10] F. Mariño, G. Baronetti, M. Jobbagy, M. Laborde, Appl. Catal. A: Gen. 238 (2003) 41.

[11] F. Haga, T. Nakajima, H. Miya, S. Mishima, Catal. Lett. 48 (1997) 223.

[12] J. Llorca, N. Homs, J. Sales, P.R. de la Piscina, J. Catal. 209 (2002) 306.

[13] J. Llorca, J.A. Dalmon, P.R. de la Piscina, N. Homs, Appl. Catal. A: Gen. 243 (2003) 261.

[14] J. Llorca, P.R. de la Piscina, J.A. Dalmon, J. Sales, N. Homs, Appl. Catal. B: Environ. 43 (2003) 355.

[15] J. Llorca, N. Homs, J. Sales, J.L.G. Fierro, P.R. de la Piscina, J. Catal. 222 (2004) 470.

[16] A. Kaddouri, C. Mazzocchia, Catal. Commun. 5 (2004) 339.

[17] J. Llorca, N. Homs, P.R. de la Piscina, J. Catal. 227 (2004) 556.

[18] J. Llorca, P.R. de la Piscina, J. Sales, N. Homs, Chem. Commun. (2001) 641.